

Rate and temperature effects on crack blunting mechanisms in pure and modified epoxies

IT-MENG LOW, YIU-WING MAI

Department of Mechanical Engineering, University of Sydney, Sydney, New South Wales 2006, Australia

The failure mechanisms of several epoxy polymers (including pure, rubber- and particulate-modified, as well as rubber/particulate hybrid epoxies) were investigated over a wide range of strain rates (10^{-6} to 10^2 sec^{-1}) and temperatures (-80 to 60°C). A substantial variation in fracture toughness, G_{Ic} , with rate was observed at both very high and very low strain rates. Under impact testing conditions, G_{Ic} for both pure and rubber-modified epoxies displayed peaks at about 23 and -80°C which appeared to correlate with the corresponding size of the crack tip plastic zone. In order to explain these rate- and temperature-dependent G_{Ic} results, two separate crack blunting mechanisms were proposed: thermal blunting due to crack tip adiabatic heating and plastic blunting associated with shear yield/flow processes. Thermal blunting was found to occur in the pure- and rubber-modified epoxies under all impact testing conditions and temperatures above 0°C . For temperatures below -20°C under impact conditions, the fracture toughness is dependent on viscoelastic loss processes and not thermal blunting. Plastic blunting was predominant at very slow strain rates less than 10^{-2} sec^{-1} for the pure- and rubber-modified epoxies and at impact strain rates for the fibre and hybrid epoxies. Microstructural studies of fracture surfaces provided some essential support for the two proposed crack blunting mechanisms.

1. Introduction

The application of linear elastic fracture mechanics parameters, critical strain energy release rate, G_{Ic} , and fracture toughness, K_{Ic} , to describe and characterize crack growth in polymers is now firmly established [1]. Because of the viscoelastic nature of polymers, sub-critical crack growth can take place at G and K levels below G_{Ic} and K_{Ic} and this depends on both rate and temperature. For a given temperature, T , the rate effect is usually expressed in terms of crack velocity, \dot{a} . Theoretical relationships between $K(G)$, \dot{a} and T have been obtained by Marshall *et al.* [2], Atkins *et al.* [3] and Mai and Atkins [4] for several glassy polymers. Various experimental techniques to determine K - \dot{a} relations have also been discussed [5]. In this work our interest is on the variation of K_{Ic} or G_{Ic} with T and applied strain rate ($\dot{\epsilon}$) or stressing rate ($\dot{\sigma}$). Low strain rates can be achieved by conducting quasi-static experiments in compact tension (CT) or single-edge notched bend (SENB) specimens in an Instron machine over a range of cross-head speeds. High strain rates are obtainable from Charpy impact specimens by either varying the impact velocity (V) or the span of the specimen (L).

Umar-Khitab *et al.* [6] have recently carried out fracture toughness experiments on polymethylmethacrylate (PMMA) using both low strain rate CT specimens and high strain rate Charpy impact test pieces. They showed that the impact toughness results could be predicted by extrapolation of the quasi-static CT toughness data to a strain rate equivalent to that

experienced during the Charpy impact tests. However, they cautioned about the change of fracture micro-mechanisms, such as thermal softening, which might affect the toughness at impact strain rates. Even under strictly impact conditions, Williams and co-workers [7, 8] have observed a very strong time (t) dependence on G_{Ic} ($\propto t^{-0.42}$) in a range of polymeric materials. Initially, the apparent increase of G_{Ic} with applied strain rate, $\dot{\epsilon}$, was ascribed to viscoelastic loss processes in the craze material at the crack tip [7]. Subsequently, this was found to be incorrect and the results were then explained in terms of crack blunting due to adiabatic heating at the crack tip [8]. A rate effect has also been observed in polymers subjected to fatigue at different frequencies. For example, hybrids due to localized adiabatic heating have been observed on fracture surfaces of epoxy resins [9]. Recently, Kinloch *et al.* [10] queried whether it was necessary to use the adiabatic heating-induced crack blunting mechanism to explain the rate dependence of G_{Ic} at impact conditions. They showed that such an effect could also be satisfactorily interpreted in terms of purely dynamic effects associated with impact testing.

Temperature has a significant effect on fracture toughness of many brittle polymers. For example in PMMA under quasi-static testing conditions, Morgan and Ward [11] found that K_{Ic} decreased with increasing temperature from -50°C to the glass transition temperature, T_g ($\sim 110^\circ \text{C}$). Mizutani [12] observed the same results and obtained K_{Ic} values at and beyond T_g . He suggested that the K_{Ic} peak at T_g was related to

the large increase in crack tip plastic zone size at this temperature. It is dubious that Mizutani's K_{Ic} results at T_g are anything but correct, for to obtain a valid K_{Ic} value at T_g the specimen thickness required would be 10 mm which is much larger than the 3 mm actually used. Putting side grooves in specimens is not usually totally sufficient to guarantee plane strain fracture [5]. In fact the variation of K_{Ic} with T can be accurately predicted from the isothermal-adiabatic transition model put forward by Williams and co-workers for glassy polymers [2, 4]. It is not necessary to resort to correlation with plastic zone size which appears to be a semi-circular argument. When T is less than -50°C and down to -197°C , Johnson and Radon [13] observed a K_{Ic} peak for PMMA at about -60°C which they proposed to agree with the presence of a β -relaxation peak at that temperature.

Although in impact testing of thermoplastics good correlation of impact toughness with viscoelastic loss processes has been observed [14], the result is not general. This has led Kisbenyi *et al.* [15] to remark that impact toughness peaks are not simply the loss $\tan \delta$ peaks transposed to some other set of conditions, but are a separate mechanism which relies on the same basic molecular relaxations. Vincent [16] has observed that the impact toughness peaks are particularly prevalent in blunt notches which appear to diminish with increasing notch sharpness. This implies that crack blunting is an important factor to be associated with variation in impact data observed. Realizing the importance of thermal effects in propagating cracks in polymers, Williams and Hodgkinson [8] proposed an adiabatic heating-induced crack blunting mechanism to account for temperature and strain rate effects on impact toughness.

The effects of strain (loading) rate and temperature on pure and rubber-modified epoxies have been investigated extensively by Young and Kinloch and their co-workers [17, 18] under quasi-static conditions using mainly CT specimens and by Scott *et al.* [19] using double torsion specimens in an Instron machine. Toughness generally decreases with strain rate with "stick-slip" fracture at low rates and continuous stable fracture at high rates. Toughness also decreases very slightly with temperature initially but increases as the glass transition temperature is approached (i.e. for $-50^\circ\text{C} < T < T_g$) [17, 18]. However, toughness has been observed to increase with decreasing temperatures for $-200^\circ\text{C} < T < -100^\circ\text{C}$ [19]. Low temperatures between -100 and 0°C favour continuous stable cracking but extremely low (i.e. less than -100°C) and high (i.e. greater than 20°C) temperatures promote "stick-slip" fracture [17-19]. These results (except the very low temperature data) are shown to be consistent with the crack blunting model put forward by Kinloch and Williams [20] and a master curve can be obtained relating G_{Ic} , time-to-failure, t_f , and test temperature by an Arrhenius equation [21]. A recent review on the mechanics and mechanisms of fracture in epoxies, both pure and rubber toughened, has been given by Garg and Mai [22]. There is little work on the effect of temperature on fracture toughness of epoxies and the associated mechanisms under

impact testing conditions. As particulate- and fibre-filled epoxies are being increasingly used in engineering applications there is also a need to understand rate and temperature effects on the fracture toughness.

In this paper we report the strain rate and temperature dependence of fracture toughness of several particulate- (short alumina fibres and metastable zirconia particles) modified and pure epoxy resins. Strain rate effects were studied using both the quasi-static SENB and CT as well as dynamic Charpy impact specimens. Temperature effects on pure and rubber-modified epoxies were investigated in the temperature range -80 to 60°C using the Charpy notched impact specimens. The influence of notch root radius on impact toughness was also studied. The observations of the results are discussed in relation to the micro-mechanisms of deformation processes at the crack tip.

2. Experimental work

The epoxy resin employed was GY250, a diglycidyl ether of bisphenol A (DGEBA) (Ciba Geigy (Aust) Pty Ltd., Sydney). The curing agent was piperidine. The rubber used was a carboxyl-terminated, random copolymer of butadiene and acrylonitrile, CTBN (1300 X13). The rigid fillers were short commercial Al_2O_3 fibres (≈ 2 mm long) and metastable ZrO_2 powders. The latter was derived from calcination of commercial purity zirconyl chloride at the appropriate temperature. The formulations of the various epoxy systems studied are shown in Table I.

The details of the preparation and testing of both unmodified and modified epoxy resins were similar to those described by Kinloch *et al.* [23]. Essentially, sheets of the material, 6 mm thick, were prepared by casting in a greased metal mould which was then heated for 16 h at 120°C to effect cure of the epoxy. In the rubber-modified epoxies the average rubber particle size was about $11.5 \mu\text{m}$. The flexural modulus was determined from three-point bend tests. The fracture toughness, G_{Ic} , was measured using the compact tension (CT) and three-point bend single-edge notched (SENB) test specimens. Tests were conducted with an Instron machine at ambient temperature and with cross-head speeds ranging from 0.05 to 20 mm min^{-1} . SENB specimens had beam depths (W) of 10 and 50 mm with normalized crack lengths (a/W) ranging between 0.1 to 0.7. The span-to-beam depth ratio was kept constant at 4 throughout the tests. The impact tests were performed on a Zwick Charpy machine with striking tups of various weights to cover

TABLE I The formulations of various epoxy polymers

Designation of various systems	Compositions (p.h.r.*)				
	epoxy	CTBN	Al_2O_3 fibre	ZrO_2	Piperidine
E	100	-	-	-	5
ER	100	15	-	-	5
EF	100	-	19	-	5
EZ	100	-	-	25	5
ERF	100	15	19	-	5
ERZ	100	15	-	25	5

*Parts per hundred resin.

a wide range of fracture energies. The tup has a striking velocity (V) of about 3.0 m sec^{-1} . The specimens used for the impact tests had constant thickness (B) of 6 mm, depth (W) of 10 mm and spans (L) of 40, 70 and 100 mm. The notch depth was varied to yield (a/W) ratios of approximately 0.1 to 0.6 in steps of 0.1. All the above specimens were notched with a sharp razor blade by either gently tapping or pushing slowly into the sawn notch in a vice. The influence of notch root radius and temperature on the impact toughness of pure epoxy (E) and rubber-modified epoxy (ER) systems was also studied. The notch tip radii for the impact test specimens varied from 0.15 to 1.5 mm and with normalized crack lengths (a/W) ranging between 0.1 and 0.6. These specimens were subjected to conditioning at 80°C for 4 h and oven cooling to room temperature prior to testing to remove any residual machining stresses. The temperature dependence of impact toughness was investigated over a temperature range -80 to 60°C .

The impact fracture toughness could be determined from the relation [7, 24]

$$U = G_c BW\phi + U_0 \quad (1)$$

where U is the measured energy, U_0 is the kinetic energy and ϕ is the calibration factor for the particular geometry used. By varying the span L , it was possible to vary the nominal strain rate ($\dot{\epsilon}$) given by

$$\dot{\epsilon} = 6 \left(\frac{V}{W} \right) \left(\frac{W}{L} \right)^2 \quad (2)$$

The value of G_{Ic} from impact tests on specimens with blunt notches was calculated from the relation [24]

$$G_B = \frac{2}{\pi} w_p R + \frac{G_{Ic}}{2} \quad (3)$$

where G_B is the "apparent" G_{Ic} value at some finite notch tip radius R , $w_p (= \sigma_y^2/2E)$ is the energy per unit volume to yield, σ_y and E are yield strength and Young's modulus, respectively.

The fracture surfaces of the tested specimens were coated with platinum and observed using a Joel 35-C scanning electron microscope to study fracture mechanisms.

3. Results

The fracture toughness, G_{Ic} , of various epoxy systems as obtained from the different types of tests and testing conditions (i.e. strain rates) are enumerated in Table II. There is a vast difference in strain rates in the various tests: Charpy impact specimens have the largest and single-edge notched bend (SENB) specimens the lowest strain rates. There appears to be a strong correlation between the fracture toughness G_{Ic} of various epoxies and strain rate. G_{Ic} generally decreases and attains a minimum value in the testing rates of compact tension specimens but increases rapidly as very fast and very slow strain rates are approached. This observation is clearly depicted in Fig. 1 for the pure epoxy (E) and rubber-modified epoxy (ER) systems. The data above $\dot{\epsilon} = 0$ are obtained from impact tests by varying the span L . The trend of these toughness data appears to

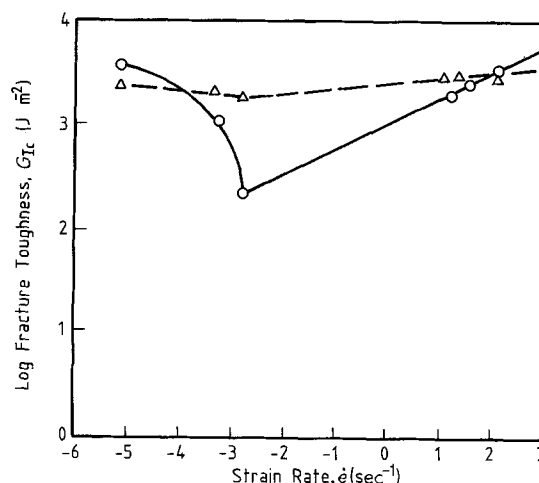


Figure 1 Variation of fracture toughness, G_{Ic} , with strain rate, $\dot{\epsilon}$, for (O) pure epoxy (E) and (Δ) rubber-modified epoxy (ER).

substantiate the results reported by Williams and co-workers [2, 3] on other polymers. However, the rate effect on fracture toughness is very different when alumina and ZrO_2 fillers are added to the epoxy matrix. Here the modified epoxies of EF, ERF and ERZ show reduced fracture resistances in impact when compared to testing in compact tension (Table II). Invariably, there is a strong correlation between microstructure modification and rate dependence on the fracture toughness of epoxies.

The degree of strain rate effects on the fracture toughness, G_{Ic} , of pure and rubber-modified epoxies may be discerned from the $\log G_{Ic} - \log \dot{\epsilon}$ plot given in Fig. 1. For the slow rate tests, i.e. $\dot{\epsilon} < 10^{-3} \text{ sec}^{-1}$, there is a negative dependence of G_{Ic} on $\dot{\epsilon}$. For the high rate impact tests, i.e. $\dot{\epsilon} > 0$, G_{Ic} increases with $\dot{\epsilon}$ according to

$$G_{Ic} \propto \dot{\epsilon}^{0.52} \quad (4)$$

for the pure epoxies, and

$$G_{Ic} \propto \dot{\epsilon}^{0.12} \quad (5)$$

TABLE II Fracture toughness of various epoxy polymers tested under various conditions

Test specimen geometry	Strain rate (sec^{-1})	System	Temp. ($^\circ \text{C}$)	Fracture toughness G_{Ic} (kJ m^{-2})
Compact tension (CT)	$\sim 1.1 \times 10^{-3}$	E	23	0.23
		ER		1.86
		EF		1.73
		EZ		0.29
		ERF		3.82
		ERZ		3.00
Single-edge notched bend (SENB)	6.5×10^{-4}	E	23	1.20
	6.5×10^{-6}	E		3.80
	6.5×10^{-4}	ER		2.40
	6.5×10^{-6}	ER		2.42
Charpy impact	18	E	23	2.43
	37	E		2.69
	113	E		3.50
	18	ER		3.04
	37	ER		3.10
	113	ER		3.30
	113	EF		1.62
	113	EZ		1.52
	113	ERF		2.50
	113	ERZ		1.83

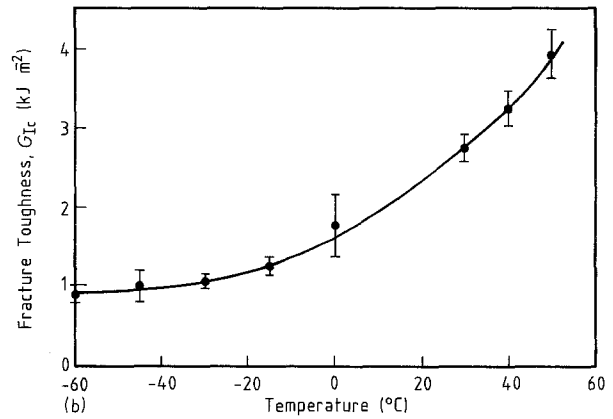
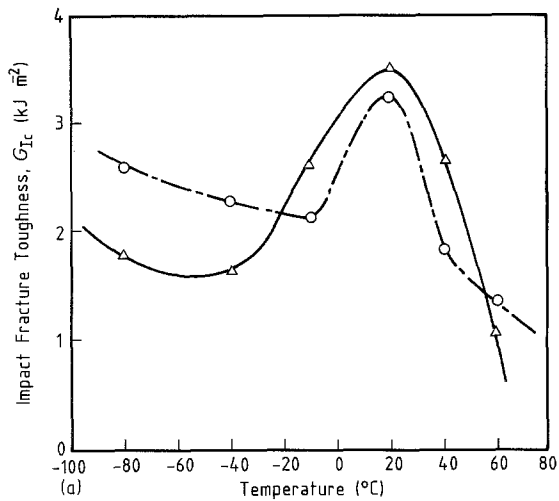


Figure 2 (a) Temperature dependence of (a) impact fracture toughness, G_{Ic} in (Δ) pure and (\circ) rubber-modified epoxies, and (b) slow rate compact tension fracture toughness, G_{Ic} in rubber-modified epoxies.

for the rubber-modified epoxies. These correlations suggest a strong rate dependence in pure epoxies but a much weaker one in the rubber-modified epoxies during impact testing. The anomalies of the rate dependence in two domains of strain rates and that between the two epoxy systems are discussed later in Section 4.

The temperature dependence of impact toughness G_{Ic} of E and ER epoxies is shown in Fig. 2a. Both epoxy systems appear to exhibit a large peak in fracture resistance at ambient temperature of 23°C which drops off rapidly with further increase in temperature. It is interesting to note that G_{Ic} values of E are significantly higher than those of ER in the temperature range -15 to $+45^\circ\text{C}$ and lower at other temperatures. Another important feature worth noting is that G_{Ic} increases with decreasing temperature for $T < -40^\circ\text{C}$. This observation appears to be in general accord with results reported by various workers [11–13] on PMMA with they attributed to viscoelastic loss processes. In the quasi-static compact tension tests on rubber-toughened epoxies, G_{Ic} increases monotonically from -60 to 60°C as shown in Fig. 2b. This trend is clearly very different to the impact toughness results in Fig. 2a. A similar trend has been observed for the toughness G_{Ic} of pure epoxies determined from low rate CT specimens. Because these results are similar to those given in [17] they are not given here.

Fig. 3 depicts the notch root radius dependence of impact toughness in both pure and rubber-modified epoxies in accordance with Equation 3. These results show that the blunter the notch root, the higher the impact resistance that can be imparted to the epoxies. This is in accord with the critical stress at a critical distance fracture criterion for blunt notches [1]. Extrapolation of the results in Fig. 3 to infinitesimal radius ($R \rightarrow 0$) simulate the fracture toughness, G_{Ic} , obtained under very sharp notch conditions. G_{Ic} values of 0.2 and 1.78 kJ m⁻² were thus obtained for E and ER epoxies which agree rather well with the compact tension derived values of 0.23 and 1.86 kJ m⁻², respectively (Table II). This means that crack blunting is small in CT specimens. However, the fact that razor sharp impact specimens displayed G_{Ic} values of 3.5 (E)

and 3.3 (ER) kJ m⁻² must mean that some enhanced processes of *in situ* notch tip blunting have taken place during impact testing.

Scanning electron microscopic studies of fracture surfaces reveal some interesting features. (i) Extensive formation of river markings near the crack initiation region in epoxies (E and ER) which showed high impact toughness, G_{Ic} , values (Fig. 4) and much less so in epoxies (EF and EZ) which displayed very low G_{Ic} values (Fig. 5). (ii) Formation of a “stretched” zone is clearly discernable in SENB specimens of E and ER (Fig. 6) when tested at a very low strain rate of $6.5 \times 10^{-6} \text{sec}^{-1}$ and not when tested at a much higher strain rate of $6.5 \times 10^{-4} \text{sec}^{-1}$. Formation of a stress-whitened zone (SWZ) is much more extensive and pronounced at the higher strain rate but some form of matrix microcracking predominates at the lower strain rate (Fig. 7). (iii) Fracture surfaces of compact tension epoxy resin composites displayed various energy dissipative deformation processes such as matrix voiding due to fracture of rubbery particles, crack pinning,

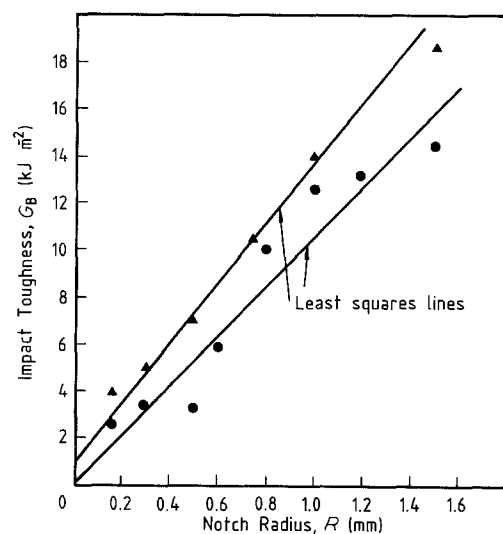


Figure 3 Notch root radius dependence of impact toughness in (\bullet) pure and (\blacktriangle) rubber-modified epoxies at ambient temperature. Least squares lines are given which show that at $R = 0$, $G_{Ic} = 1.78$ and 0.2 kJ m⁻² for ER and E, respectively.

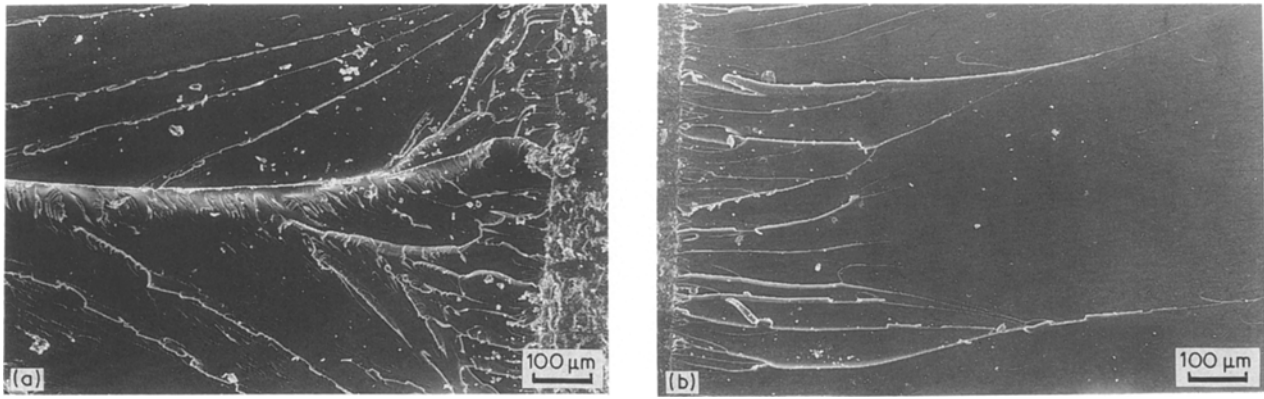


Figure 4 Fracture surfaces of (a) E and (b) ER impact tested at ambient temperature ($\dot{\epsilon} = 10^2 \text{ sec}^{-1}$).

fibre–matrix debonding, fibre deformation and fracture, fibre pull-out, fibre bridging of crack surfaces, localized plastic shear deformations, etc. (Fig. 8). (iv) Blunt notch impact tested specimens revealed the characteristic brittle fracture surfaces with the origin of fracture initiation clearly identified (Fig. 9). The presence of the rubber particles appears to have resulted in the hyperbolic markings during unstable fracture of the ER material. The density of these hyperbolic markings is larger for those notched samples with a larger notch radius and hence a higher initiation fracture toughness. That such hyperbolic markings are not seen in the pure epoxies may suggest that the rubber dispersions act as sites for secondary crack initiations.

4. Discussion

The correlation between fracture properties and microstructures of compact tested pure and modified epoxies has already been discussed elsewhere [25]. In essence, the primary source of toughening operating in rubber-modified epoxies and hybrids derives from the greater extent of plastic-shear deformations around the crack tip which results in a more pronounced stress intensity reduction (i.e. blunting) during crack propagation. This phenomenon is greatly enhanced in the hybrids where the presence of rigid particles or fibres serves to promote repeated or multiple crack tip blunting with the concomitant formation of a larger stress-whitened zone (SWZ) and stabilization of slow crack growth [26]. All these processes contribute to a greater fracture resistance,

G_{Ic} , achieved by the CT and SENB tested hybrids (ERZ and ERF) and vice versa in impact tests where high strain rates are not conducive for localized plastic-shear deformations.

The data presented in Figs 1 and 2 clearly show that there is a strong rate and temperature dependence of impact toughness in E and ER systems. The question now centres on the underlying origins of this observed strong dependence in these materials and these are discussed below.

4.1. Evidence of crack tip blunting

The concept of crack tip blunting was originally proposed by Kinloch and Williams [20] to explain unstable “stick–slip” fractures observed in epoxies under quasi-static conditions. Blunting occurs as a direct result of plastic shear flow at the crack tip. Evidence in support of this mechanism is given in Fig. 6 which shows the “stretched zone” formed at crack initiation in E and ER materials tested with SENB specimens at ambient temperature. A “stretched zone” can only be formed if there is plastic flow and blunting of the sharp crack tip. Under impact or very high strain rate testing conditions, Williams and Hodgkinson [8] suggested adiabatic crack tip heating to be responsible for crack blunting in a range of polymers. We concur with this view for the following observations.

(a) The straight line relationship between G_B and R for blunt notch Charpy specimens in Fig. 3 may be used as calibration curve to estimate crack tip blunting radius, R , for sharp notch impact tested samples. In

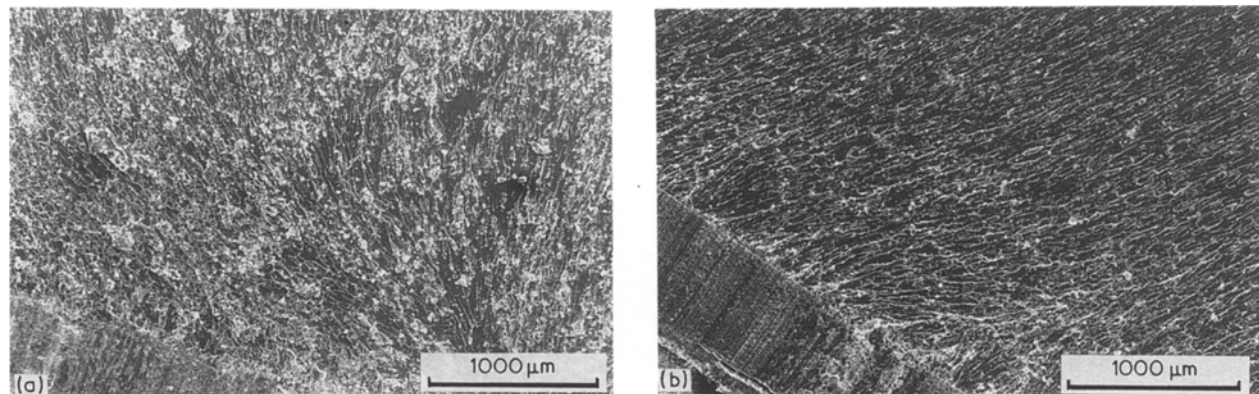


Figure 5 Fracture surfaces of (a) EF and (b) EZ impact tested at 23°C ($\dot{\epsilon} = 10^2 \text{ sec}^{-1}$).

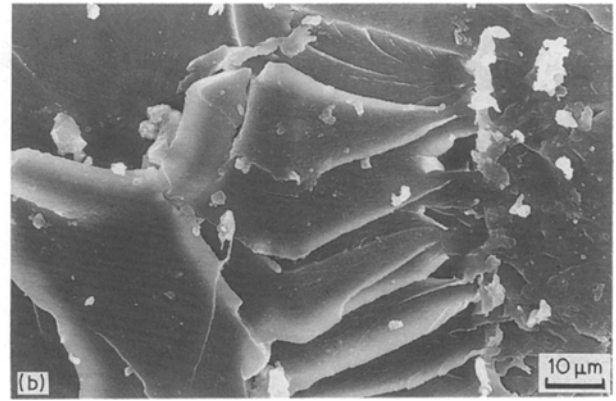
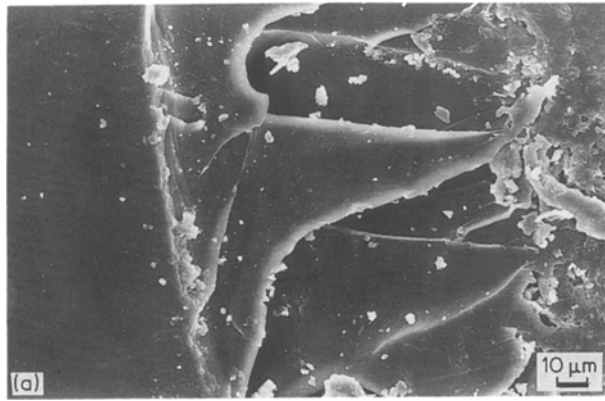


Figure 6 Formation of a “stretched” zone in the SENB specimens of (a) E and (b) ER tested at $\dot{\epsilon} = 6.5 \times 10^{-6} \text{sec}^{-1}$ and ambient temperature.

Table II the G_{Ic} values for the pure and modified epoxies at ambient temperature and $\dot{\epsilon} = 113 \text{sec}^{-1}$ are 3.50 and 3.30 kJ m^{-2} , respectively. Using these G_{Ic} values and Fig. 3 we can estimate the equivalent crack tip radii due to thermal blunting to be 300 and 200 μm , respectively. Had the crack tip remained sharp the G_{Ic} values would have been much lower and equal to 0.2 and 1.78 kJ m^{-2} for these respective materials. (See G_B in Fig. 3 when $R = 0$.)

(b) That thermal blunting and not plastic blunting is the major reason for the high toughness values in the notched impact tested pure and rubber-modified epoxies can be confirmed by estimating the temperature rise (ΔT) at crack initiation from the expression [8]

$$\Delta T = G_{Ic}/(\pi \rho c k t)^{1/2} \quad (6)$$

where ρ is the density, c is the specific heat, k is the thermal conductivity and t is the loading time. Consider the pure epoxy; we have $G_{Ic} = 3.5 \text{kJ m}^{-2}$, $t \approx 0.4 \text{msec}$ and $\pi \rho c k \approx 2.3 \times 10^6 \text{J}^2 \text{sec}^{-1} \text{m}^{-4} \text{K}^{-2}$ so that at $\Delta T \approx 115^\circ \text{C}$. This temperature rise is well above the softening temperature of the pure epoxy which is approximately 100°C as measured by differential scanning calorimetry (DSC) technique. A similar temperature rise is predicted for the rubber-modified epoxies whose softening temperature is about 88°C . Thermal blunting is therefore the most significant source of high toughness in impact tested epoxies. There is clear evidence of a “stretched zone”, approximately 200 μm in length (which is less than the

predicted 300 μm from Fig. 3), in the pure epoxy resin in Fig. 4 to support this thermal blunting mechanism.

(c) In the blunt notch impact analysis of Williams and Hodgkinson [8] a parameter N is defined to distinguish two separate crack tip blunting mechanism, i.e.

$$N = (e_y/2)^{1/2} (\sigma_c/\sigma_y) \quad (7)$$

When $N < 0.71$ thermal blunting occurs, but when $N \geq 0.77$ self blunting can occur without thermal effects, i.e. blunting occurs by other plastic flow processes. Because σ_y decreases with temperature, e_y and σ_c are approximately constant, N will increase with increasing temperature, thus changing the thermal blunting mechanism to self blunting above some critical temperature. For the ambient temperature notched impact tests, using $\sigma_c = 340 \text{MPa}$, $e_y = 0.03$ and $\sigma_y = 88 \text{MPa}$ for the pure epoxy and corresponding values of 200 MPa, 0.025, and 68 MPa for the rubber-modified epoxy [25], we can calculate N equal to 0.45 and 0.33 for these two epoxy materials. These N values are less than the critical value of 0.71 thus indicating thermal blunting has taken place during the impact tests.

(d) Under slow rates a stress-whitened or damaged zone of material is developed ahead of the crack tip in the rubber-modified epoxies. This is due to the cavitation and debond of rubber particles which subsequently initiate a predominant shear deformation mechanism in the epoxy matrix. However, under impact testing conditions, the rubber-modified epoxies

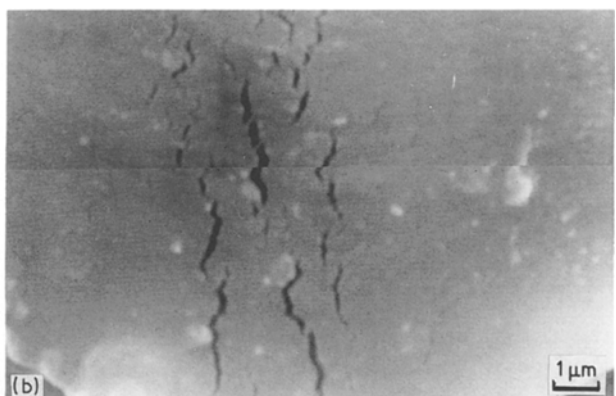
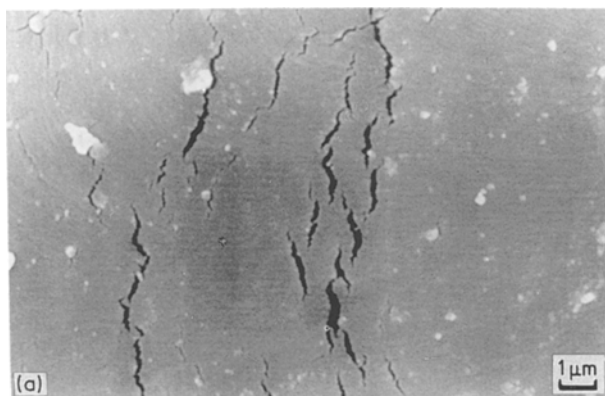


Figure 7 Formation of matrix microcracks within the “stretched zones” in the SENB specimens of (a) E and (b) ER tested at $\dot{\epsilon} = 6.5 \times 10^{-6} \text{sec}^{-1}$.

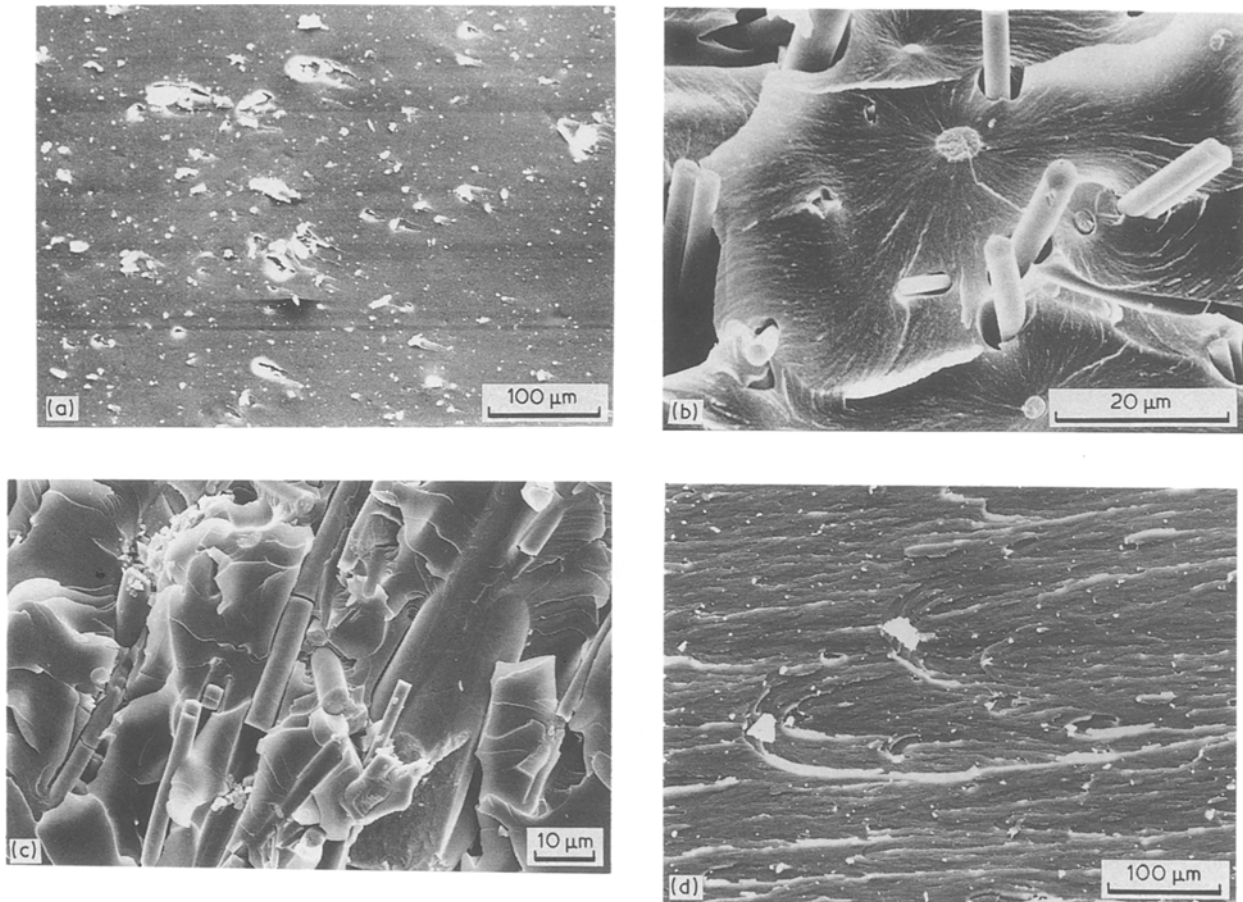


Figure 8 Various fracture processes in modified epoxy systems tested at $T = 23^{\circ}\text{C}$ and $\dot{\epsilon} = 10^{-3}\text{sec}^{-1}$: (a) EZ, (b) ERF, (c) EF and (d) ERZ.

do not display any stress-whitened zone indicating that rubber particles do not play a significant role at very high strain rates. The approximately equal G_{Ic} values given in Table II for the pure and rubber-modified epoxies at $\dot{\epsilon} = 113\text{sec}^{-1}$ support the view that the same deformation mechanism operates in both materials. Clearly, such a mechanism can only be the thermal blunting mechanism and not plastic blunting.

Kinloch *et al.* [23] have recently put forward another reason for the high fracture toughness observed for pure and rubber-modified epoxies in impact testing, namely dynamic effects instead of thermal blunting. They showed that G_{Ic} is primarily determined by the time-to-failure (t) (which is also true for the thermal blunting mechanism) and that G_{Ic} is large if t is small and the “true” impact fracture energy can only be obtained if t is large when dynamic effects are negligible. While dynamic effects have been shown to give high fracture toughness at short failure times because the actual energy absorption in crack initiation is overestimated, it is also obvious from the observations recorded above that crack blunting due to adiabatic heating has also occurred. Dynamic effects alone cannot explain thermal blunting in the form of stretched zones found at the crack tip. Indeed the only satisfactory solution is to calculate the dynamic K_{Ic} based on the crack initiation load for a given crack length as recorded by the instrumental tup. K_{Ic} can then be used to convert to G_{Ic} through the dynamic Young’s modulus. In principle this is easy, but in practice it may be difficult to locate precisely the crack initiation

load. We suspect that the dynamic K_{Ic} and hence G_{Ic} would be larger under these impact testing conditions not only due to dynamic effects but largely due to thermal blunting of the crack tip. We have not performed any instrumented Charpy impact tests in this work but we are proceeding in this direction to measure dynamic K_{Ic} and G_{Ic} values to prove thermal blunting does exist. However, we do agree that the high G_{Ic} values in short-time impact tested specimens measured from the energy loss after impact can be due to dynamic effects and crack tip thermal blunting operating simultaneously. To exclude thermal blunting as a likely mechanism of toughening is perhaps premature.

It may be of interest to point out that in the artificially blunted notched Charpy specimens the fracture surfaces are brittle in nature with the origins of fracture initiation distinctly shown in Fig. 9. Such a fracture morphology seems to indicate that thermal blunting is little or does not occur in these blunt notch samples. In impact tests on blunt notched rubber-modified nylon specimens ($R = 0.25\text{mm}$) Wu [27] has measured a temperature rise of only 10°C which is certainly not sufficient to cause thermal blunting. Unlike the rubber-modified epoxies, however, a stress-whitened zone width (h) of about 3.0mm was observed in Wu’s experiments. Equation 6 cannot be applied in this case to calculate ΔT because it is derived based on $h \rightarrow 0$. For $h \neq 0$ the adiabatic temperature rise at the crack tip can be calculated from [8]:

$$\Delta T = \frac{G_{Ic}}{qch} \left\{ 1 - 4i^2 \operatorname{erfc} \left[\frac{h^2 qc}{16kt} \right]^{1/2} \right\} \quad (8)$$

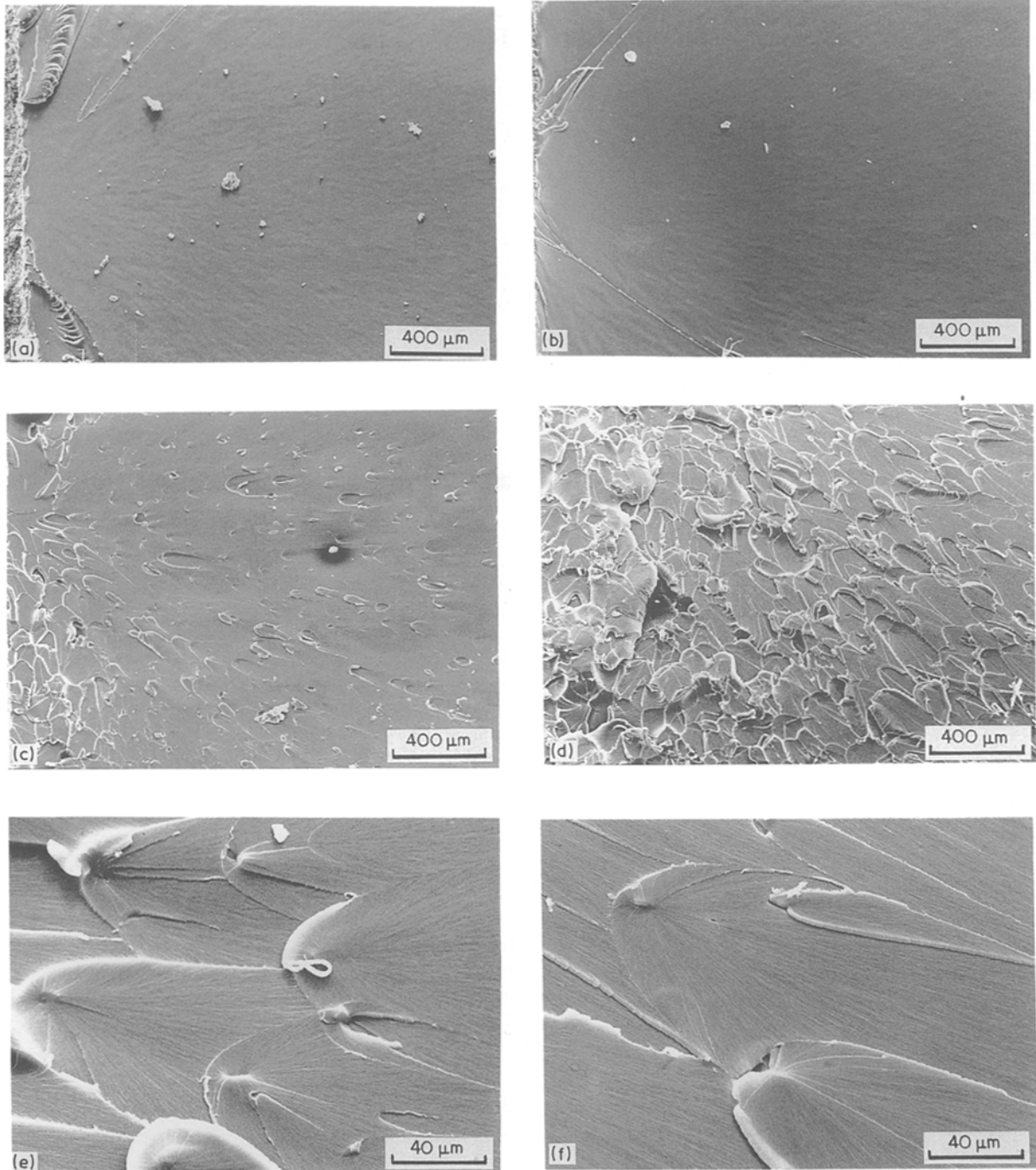


Figure 9 Fracture surfaces of blunt notch impact tested E and ER specimens: (a) E ($R = 0.3$ mm), (b) E ($R = 0.63$ mm), (c) ER ($R = 0.3$ mm), (d) ER ($R = 0.75$ mm); hyperbolic markings on fracture surfaces of ER (e) $R = 0.3$ mm and (f) $R = 0.75$ mm.

From Wu's experiments we have $G_{Ic} \approx 88 \text{ kJ m}^{-2}$, $h \approx 3.0 \text{ mm}$, $\rho = 1087 \text{ kg m}^{-3}$, $c = 1.6 \text{ J g}^{-1} \text{ K}^{-1}$, $k = 0.2 \text{ W m}^{-1} \text{ K}^{-1}$ and $t \approx 0.85 \text{ sec}$. Thus, $\Delta T \approx 17^\circ \text{C}$ (which is close to the experimental value of 10°C) and this is not sufficient to induce thermal blunting. Nonetheless, this moderate temperature rise has promoted considerable matrix yielding in the nylon material to give a high fracture toughness.

4.2. Effects of temperature and strain rate on fracture toughness

4.2.1. Temperature effect

Fig. 2 shows the variation of fracture toughness, G_{Ic} , of the pure and rubber-modified epoxies under Charpy impact and quasi-static compact tension testing conditions. The monotonic rise in G_{Ic} with tem-

perature in the CT specimens, Fig. 2, is primarily due to the increasing amount of crack tip blunting as the yield stress is decreased when temperature increases. Adiabatic heating does not play any role in the blunting mechanism in these slow strain rate experiments. As the glass transition temperature is approached fracture will become more ductile and eventually the linear elastic fracture mechanics parameters K_{Ic} and G_{Ic} are no longer useful.

Under impact testing high strain rate ($\dot{\epsilon} \approx 10^2 \text{ sec}^{-1}$) conditions, the fracture toughness, G_{Ic} given in Fig. 2a shows a peak at about 20°C and it has a tendency to rise with decreasing temperature at below -30°C . In order to explain these impact toughness results we note that from DSC measurements there are two $\tan \delta$ peaks at about 100 and -75°C for the pure epoxies

and 90 and -70°C , respectively, for the rubber-modified epoxies. Clearly, there is no one-to-one correspondence between the G_{Ic} peak and the loss $\tan \delta$ peak at the high temperature end. In Section 4.1 we have already indicated that adiabatic heating would induce crack tip blunting by softening a zone of material prior to unstable crack propagation. The whole process is to increase the impact fracture toughness as would be measured from an effectively higher test temperature (which is equal to the sum of the ambient temperature and the adiabatic temperature rise, ΔT). However, we cannot explain the reduction in G_{Ic} as the test temperature is increased to 40 and 60°C . The effective test temperature would be well above the softening temperature but the fracture was still essentially brittle so that G_{Ic} could be obtained with Equation 1. It is unlikely that thermal embrittlement could have resulted in the low G_{Ic} values for these materials because the loading time is of the order of milliseconds.

At the low temperature end (less than -20°C) the adiabatic temperature rise is not sufficient to cause thermal blunting. Consequently, G_{Ic} should decrease with decreasing temperature providing no other relaxation processes exist. However, Fig. 2a shows that the reverse is true. Because there is a loss peak at about -70°C for both materials we suggest that the viscoelastic loss of this β -transition in the temperature range -30 to -100°C is solely responsible for the increasing G_{Ic} observed. The β -transition is believed to involve the relaxation of hydroxy-ether groups in the network [28] which allows some limited flow processes to take place at the crack tip. Heat is usually evolved with the β -relaxation which, in principle, helps in softening and blunting the crack tip. This hypothesis is based on the observation of microwave sintering and curing of thermoset resins [29, 30] whereby microwaves are used to continually induce relaxations of molecular chains with the concomitant release of heat to enable the conventional cross-linking and curing of resins to commence. However, at these very low temperatures the temperature rise is not high enough to cause thermal blunting to occur. Even so, the visco-

elastic loss processes due to the β -transition would still contribute to the total fracture toughness, G_{Ic} .

The plastic zone size, r_p , at the crack tip can be modelled by the Dugdale model [1] and this gives

$$r_p = \frac{\pi}{16} \left(\frac{G_{Ic}}{w_p} \right) \quad (9)$$

where w_p can be obtained from Equation 3 using the impact blunt notch data of Fig. 3, i.e. $w_p = 16.7 \times 10^6$ and $19.2 \times 10^6 \text{ J m}^{-3}$ for the pure and rubber-modified epoxies, respectively. Because w_p does not vary significantly but remains roughly constant with temperature we can evaluate r_p as a function of temperature using Equation 9. These r_p results are plotted in Fig. 10 and it is clearly shown that there is a one-to-one correspondence with the G_{Ic} results in Fig. 2a, i.e. the r_p and G_{Ic} peaks match each other. This observation is expected and cannot be used to justify the G_{Ic} -temperature data.

4.2.2. Strain rate effect

From Fig. 1 it is obvious that the rubber-modified epoxies are less dependent on strain rates than the pure epoxies, and for each material the strain rate dependence of G_{Ic} is negative for quasi-static CT and SENB tests, but this dependence becomes positive for the Charpy impact tests. Such apparent contradictory behaviour originates from the two different crack blunting mechanisms operating in each domain of strain rates. In the high rate impact test domain, thermal blunting due to localized adiabatic heating at the crack tip causes G_{Ic} to increase with $\dot{\epsilon}$. Because $\dot{\epsilon} \propto t^{-1}$ we expect G_{Ic} to vary inversely with t or proportionally with $\dot{\epsilon}$. For the pure epoxies, $G_{Ic} \propto \dot{\epsilon}^{0.52}$ ($\propto t^{-0.52}$) and this agrees well with the inverse square root time dependence of G_{Ic} for small N values as predicted by Williams and Hodgkinson [8]. For the rubber-modified epoxies, $G_{Ic} \propto \dot{\epsilon}^{0.12}$ ($\propto t^{-0.12}$). Although this is not as strong a time dependence, the mechanism of increasing G_{Ic} with $\dot{\epsilon}$ is still one of thermal blunting.

In the low strain rate CT and SENB domain, the negative rate dependence of G_{Ic} is entirely a result of the plastic blunting mechanism. Plastic blunting obviously decreases with increasing strain rate because of the increasing yield strength. Adiabatic heating does not play any part in crack tip blunting here. A close examination of Fig. 6 shows that "stretched zones" are formed during crack initiation in both E and ER materials. The sizes of these zones (s) at $\dot{\epsilon} = 6.5 \times 10^{-6} \text{ sec}^{-1}$ are, respectively, 120 and $90 \mu\text{m}$ for E and ER. The corresponding yield strengths, σ_y , are 75 and 55 MPa [25]. Now, as $G_{Ic} \propto \sigma_y s$, we can easily show that G_{Ic} (pure epoxy)/ G_{Ic} (rubber-modified epoxy) ≈ 1.82 which compares rather well with 1.57 ($= 3.8/2.42$) from measured G_{Ic} values given in Table II. The stretched zone size decreases more rapidly with rate (Fig. 11) than yield strength increases in the pure epoxies and this leads to G_{Ic} decreasing with the rate in these CT and SENB experiments. Because $\sigma_y s$ does not decrease significantly with rate for the rubber-modified epoxies, G_{Ic} is not expected to change very much with rate.

Notch tip blunting due to plastic flow is always

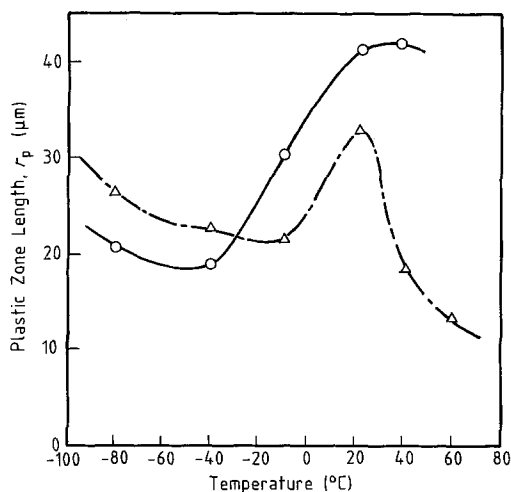


Figure 10 Variation of plastic zone size, r_p , with temperature for (O) pure and (Δ) rubber-modified epoxies under impact testing conditions.

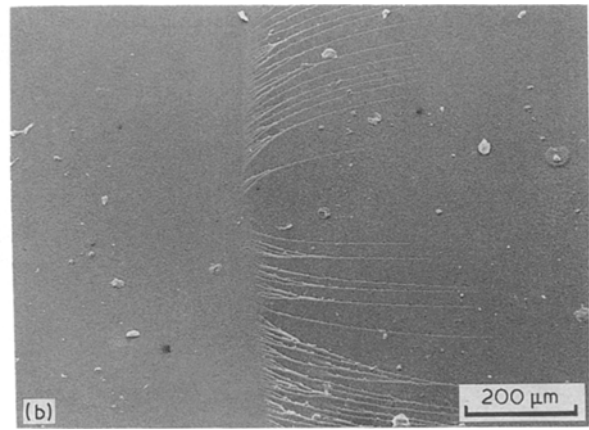
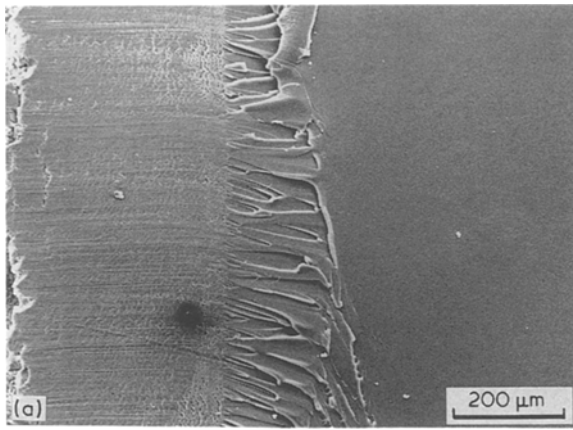


Figure 11 Effect of strain rate on stretched zones formed in pure epoxies (SENB). (a) A stretched zone formed at a cross-head speed of 10 mm min^{-1} ; and (b) absence of a stretched zone at 200 mm min^{-1} .

accompanied by large plastic strains at the crack tip initiation region in the form of a stretched zone (Fig. 6). The presence of these intense plastic strains is believed to have caused the development of matrix microcracks inside the stretched zone of the E and ER materials (Fig. 7).

Another interesting observation in these rate experiments is with the EF, ERF and ERZ materials whose high rate Charpy impact fracture toughnesses are actually smaller than the slow rate CT and SENB values. The incorporation of the ceramic fibres and particulates in the epoxy/epoxy rubber matrix appears to have suppressed the adiabatic heating induced crack blunting mechanism because of the approximately two orders of magnitude increase in the thermal conductivity, k , of these ceramic materials. If k for the composite material is considerably increased but ρ and c remain approximately unchanged then, ΔT from Equation 6 becomes small and is insufficient to cause thermal blunting due to softening. We believe that little thermal blunting, if any, occurs in EF, ERF and ERZ even under high rate impact testing conditions. The significant fracture mechanism is one of plastic blunting. Therefore, the impact fracture toughness is smaller than the low rate CT and SENB tests because of the small plastic blunting at these very high rates. Much work at other impact rates is needed on these filled epoxies to confirm our hypothesis.

5. Conclusions

A strong strain rate and temperature dependence was observed for the fracture toughness of pure and rubber-modified epoxies. Two separate crack blunting mechanisms were proposed to account for the fracture toughness data. The first mechanism involves thermal blunting due to adiabatic heating at the crack tip and it occurs under impact testing conditions for all temperatures studied. At the high temperature range above 0°C , thermal blunting increases the impact toughness corresponding to an effectively higher test temperature. However, at the low temperature range below -20°C , the adiabatic temperature rise is not sufficient to cause softening and G_{Ic} increases with decreasing temperature owing to viscoelastic losses associated with the β -relaxation there. The second mechanism involves plastic blunting due to shear

yield/flow processes at the crack tip and this takes place at slow strain rate testing of the CT and SENB samples. It also appears that even under impact testing conditions the alumina/epoxy, alumina/rubber/epoxy and zirconia/rubber/epoxy materials exhibit plastic blunting rather than thermal heating.

Acknowledgements

We thank Mr L-S. Chen for his assistance in analysing the impact toughness data and Dr S. Bandyopadhyay for supplying some of the scanning electron micrographs. We also thank the Australian Department of Defence for awarding a Postdoctoral Fellowship to one of us (I-M. Low) and the Sydney University Electron Microscope Unit for placing its facilities at our disposal.

References

1. J. G. WILLIAMS, "Fracture Mechanics of Polymers", (Ellis Horwood/John Wiley, Chichester, 1984).
2. G. P. MARSHALL, H. COUTTS and J. G. WILLIAMS, *J. Mater. Sci.* **9** (1974) 1409.
3. A. G. ATKINS, C. S. LEE and R. M. CADDELL, *ibid.* **10** (1975) 1381.
4. Y.-W. MAI and A. G. ATKINS, *Polym. Engng Sci.* **16** (1976) 400.
5. A. G. ATKINS and Y.-W. MAI, "Elastic and Plastic Fracture" (Ellis Horwood/John Wiley, Chichester, 1985).
6. S. A. UMAR-KHITAB, D. McCAMMOND and R. D. VENTER, *Polym. Engng Sci.* **25** (1985) 1035.
7. M. W. BIRCH and J. G. WILLIAMS, *Int. J. Fract.* **14** (1978) 69.
8. J. G. WILLIAMS and J. M. HODGKINSON, *Proc. R. Soc. Lond.* **A375** (1981) 231.
9. J. A. MANSON, R. W. HERTZBERG, G. M. CONNELLY and J. HWANG, in "Multicomponent Polymer Materials", edited by C. K. Riew and J. K. Gilham, Advances in Chemistry Series 210 (American Chemical Society, Washington, 1986) p. 291.
10. A. J. KINLOCH, G. A. KODOKIAN and M. B. JAMARANI, *J. Mater. Sci.* **22** (1987) 4111.
11. G. P. MORGAN and I. M. WARD, *Polymer* **18** (1977) 87.
12. K. MIZUTANI, *J. Mater. Sci. Lett.* **6** (1987) 915.
13. F. A. JOHNSON and J. C. RADON, *J. Polym. Sci. Chem. Edn* **11** (1973) 1995.
14. J. HEIJBOER, *J. Polym. Sci. (c)* **16** (1968) 3755.
15. M. KISBENYI, M. W. BIRCH, J. M. HODGKINSON and J. G. WILLIAMS, *Polymer* **20** (1979) 1289.
16. P. J. VINCENT, *ibid.* **15** (1974) 111.
17. S. YAMINI and R. J. YOUNG, *ibid.* **18** (1977) 1075.

18. A. J. KINLOCH, S. J. SHAW, D. A. TOD and D. L. HUNSTON, *ibid.* **24** (1983) 1341, 1355.
19. J. M. SCOTT, G. WELLS and D. C. PHILLIPS, "Low temperature crack propagation in an epoxy resin", UKAEA Harwell Report AERE-R 9382, May 1979.
20. A. J. KINLOCH and J. G. WILLIAMS, *J. Mater. Sci.* **15** (1980) 987.
21. A. J. KINLOCH, in "Advances in Polymer Science", Vol. 72, edited by K. Dusek (Springer-Verlag, Berlin, 1986) pp. 45-67.
22. A. C. GARG and Y.-W. MAI, *Comp. Sci. Technol.* **31** (1988) 179.
23. A. J. KINLOCH, D. L. MAXWELL and R. J. YOUNG, *J. Mater. Sci.* **20** (1985) 4169.
24. E. PLATI and J. G. WILLIAMS, *Polym. Engng Sci.* **15** (1975) 470.
25. I.-M. LOW, Y.-W. MAI, S. BANDYOPADHYAY and V. M. SILVA, *Mater. Forum* **10** (1987) 241.
26. I.-M. LOW and Y.-W. MAI, *Comp. Sci. Technol.* **33** (1988) 191.
27. S. WU, *J. Polym. Sci. Polym. Phys. Edn* **21** (1983) 699.
28. M. OCHI, M. YOSHIZUMI and M. SHIMBO, *ibid.* **25** (1987) 1817.
29. B. SILINSKI, C. KUZMYCZ and A. GOURDENNE, *Eur. Polym. J.* **23** (1987) 273.
30. M. TEFFAL and A. GOURDENNE, *ibid.* **19** (1983) 543.

*Received 10 March
and accepted 25 July 1988*